APPLICATIONS OF
MODELLING AND SIMULATION
http://arqiipubl.com/ams eISSN 2600-8084 VOL 4, 2020, 47-56

# Simulation of Wind Energy System Employing Doubly Fed Induction Generator

Stephen Ejiofor Oti[1*], Nnadi Damian Benneth[1], Ogbuefi Uche[1], Nnamani Stella[1] and Agada Stephen[2]

[1]Department of Electrical Engineering, University of Nigeria, Nsukka, Enugu State, Nigeria
[2]Department of Electrical/Electronic Engineering, Michael Okpara University of Agriculture, Umudike Abia State, Nigeria

[*]Corresponding author: stephen.oti@unn.edu.ng

*Received 12 September 2019, Revised 19 October 2019, Accepted 31 October 2019.*

**Abstract:** This work is based on the dynamics of wind energy generation considering the wind speed and the control of the rotor speed using vector control of the converters. The converters are both connected to the rotor side and grid side of the doubly fed induction generator (DFIG), pulse width modulated (PWM) generators powering the switches are controlled using various vector transformation and proportional integral (PI) control of the direct and quadrature current and the speed of the rotor. It is found that at an average wind speed of about 8.5 m/s a considerable voltage and current characteristic is evolved whereas at wind speed of about 2 m/s, the amount of voltage generated is seen not to compare favorably to the former. The modelling and simulation of this work was done using MATLAB and Simulink software.

Keywords: Doubly fed; Induction generator; Modelling; Wind energy; Wind speed.

## 1. INTRODUCTION

Wind power generation is an attractive and clean source of energy with environmentally friendly production and sustainable living using green power [1,2,3,4]. The use of fossil fuels has been creating serious environmental problems, such as gas emissions, air pollution and climate changes thereby making current energy trends to be unsustainable thus necessitating a better balance between energy, economics, development and protection of the environment [3,5].

Wind energy is one of the fastest growing sectors in renewable energy. The resources are freely available throughout the world and wind energy is mainly used for two purposes namely irrigation and electricity generation [2,6,7,8]. Winds are essentially caused by the solar heating of the atmosphere, and they carry enormous quantity of energy. Before the development of electric power on large scale, wind power has served many countries as source of power in early days, known as windmills [9]. The doubly fed induction generator (DFIG) consists of a 3-phase wound rotor and a 3-phase wound stator. The rotor is fed with a 3 phase AC signal which induces an AC current in the rotor windings. As the wind turbines rotate, they exert mechanical force on the rotor, causing it to rotate. As the rotor rotates the magnetic field produced due to the AC current also rotates at a speed proportional to the frequency of the AC signal applied to the rotor windings. As a result, a constantly rotating magnetic flux passes through the stator windings which cause induction of AC current in the stator winding. Thus the speed of rotation of the stator magnetic field depends on the rotor speed as well as the frequency of the AC current fed to the rotor windings. The basic requirement for the electricity generation using wind energy is to produce AC signal of constant frequency irrespective of the wind speed. In other words, the frequency of the AC signal generated across the stator should be constant irrespective of the rotor speed variations. To achieve this, the frequency of AC signal applied to the rotor windings need to be adjusted.

Wind energy had been exploited for thousands of years. The oldest applications of wind energy include extracting water from wells, making flour out of grain, and other agricultural applications. In recent times, the use of wind energy has evolved to, primarily, electricity generation [10]. A wind turbine is a device for extracting kinetic energy from the wind. By removing, some of its kinetic energy the wind must slow down but only that mass of air, which passes through the rotor disc, is affected. Assuming that the affected mass of air remains separated from the air, which does not pass through the rotor disc and does not slow down, a boundary surface can be drawn containing the affected air mass and this boundary can be extended upstream as well as downstream forming a long stream-tube of circular cross section [11]. Wind turbine energy generation depends on the interaction between the rotor and the wind. The wind may be considered to be the combination of the mean wind and turbulent fluctuations about the mean flow. Experience has shown that the major aspects of wind turbine performance which are mean power output and mean loads, are determined by the aerodynamic force generated by the mean wind. Periodic aerodynamic forces caused, by wind shear, off-axis winds, and rotor rotation and randomly fluctuating forces induced by turbulence and dynamic effects are the source of fatigue loads and are a factor in the peak loads experienced by a wind turbine [12].

A paper [13] dealt with the introduction of doubly fed induction generator, AC/DC/AC converter control and finally the SIMULINK/MATLAB simulation for isolated induction generator as well as for grid connected DFIG. Also, [14] worked on

three different models that were compared in terms of dynamic behavior and simulation time. However, in this paper, the particular interests are to study the response to specified wind speeds with particular reference to the rotor side and grid side and also to look at fault response in the model.

## 2. METHODOLOGY

Figure 1 represents a wind energy system linked by the converters [15]. A method of controlling wind turbine speed is to accept whatever frequency the generator produces, convert it to DC, and then convert it to AC at the desired output frequency using an inverter. This is common for small house and farm wind turbines. But the inverters required for megawatt scale wind turbines are large and expensive. In Figure 1, doubly fed generators are another solution to this problem. Instead of the usual field winding fed with DC, and an armature winding where the generated electricity comes out, there are two three-phase windings, one stationary and one rotating, being a doubly fed, both separately connected to equipment outside the generator. One winding is directly connected to the output, and produces 3-phase AC power at the desired grid frequency. The other winding usually called the field, but here both windings can be outputs, is connected to 3-phase AC power at variable frequency. This input power is adjusted in frequency and phase to compensate for changes in speed of the turbine. Adjusting the frequency and phase requires an AC to DC to AC converter. This is usually constructed from very large insulated gate bipolar transistors (IGBT) semiconductors. The converter is bidirectional, and passes power in either direction. Power can flow from this winding as well as from the output winding [16].

### 2.1 Conversion and Operation Principles

Here, discussion is on the way the AC-DC-AC converters are used on the system. It consists of two voltage-sourced converters, namely, the rotor-side converter (RSC) and the grid-side converter (GSC), which are connected "back-to-back." In between the two converters is a DC-link capacitor placed, as energy storage, in order to limit the voltage variations in the DC-link voltage. The control of the torque or the speed of the DFIG is achieved using rotor-side converter and that of the power factor at the stator terminals. The steady DC-link voltage occasioned by the grid side converter prepares it against the effects of rotor power magnitude and direction of the rotor power. The grid-side converter derives from the grid frequency to be able to deal with amount of reactive power. The rotor-side converter does not trace the grid frequency but enjoins any frequency as may arise as a function of the wind speed. The back-to-back arrangement of the converters provides a mechanism of converting the variable voltage, variable frequency output of the generator (as its speed changes) into a fixed frequency, fixed voltage output compliant with the grid [17].

The DC link capacitance is an energy storage element that provides the energy cushion required between the generator and the grid. The DFIG power electronics is composed of a two-level six switch converter. This means that the number of voltage levels that can be produced at the output of each bridge leg of the converter is two, the zero volts or the voltage of the DC link (Vdc). Figure 1 shows the connection in a back-to-back arrangement with a DC link between the two converters. The switching elements are represented by power converters IGBTs. The six-switch converter yields a three-phase output voltage which can be of arbitrary magnitude, frequency and phase. It is also such that the Vdc is greater than the peak line voltage. The synthesis and switching processes are also discussed in details in [18] as the limit is related to the switching frequency of the pulse-width modulated switching devices. At a fixed frequency the converters are switched either way and the output voltage is controlled when pulse-width is varied.

### 2.2 Aerodynamic Model

The aerodynamic model of a wind turbine can be seen in the subsequent equations. Considering wind speed and cross sectional area of the wind turbine blade, the wind power is given by [12,15]:

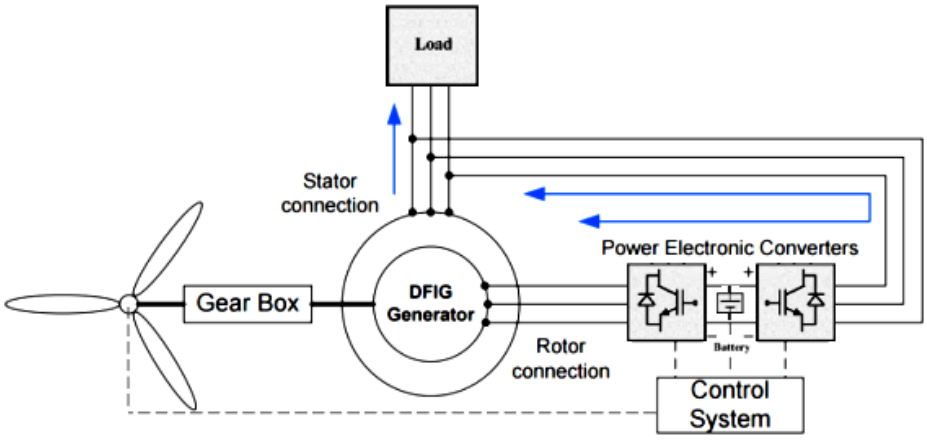


Figure 1. Induction machine (DFIG) based wind turbine

$$P_w = \frac{1}{2}\rho A V_w^3 \tag{1}$$

$$A = \pi r^2 \tag{2}$$

where $V_w$ is the wind speed (m/s), $A$ is the crossing surface area (m$^2$), $r$ is the radius of the rotor blades (m) and $\rho$ is the air density = 1.22 kg/m$^3$ at 15°C and normal pressure.

A numerical approximation of the aerodynamic power coefficient $C_p$ is given by the following equations:

$$C_p(\lambda,\beta) = c_1\left(\frac{c_2}{\lambda_i} - c_3\beta - c_4\right) exp\left(\frac{-c_5}{\lambda_i}\right) \tag{3}$$

$$\lambda_i = \left(\frac{1}{\lambda + c_6\beta} - \frac{c_7}{\beta^3 + 1}\right)^{-1} \tag{4}$$

where $c_1$ = 0.39, $c_2$ = 116, $c_3$ = 0.4, $c_4$ = 5, $c_5$ = 16.5, $c_6$ = 0.089, $c_7$ = 0.035 and $\beta$ is the pitch angle. The effective mechanical power $P_m$ which is transferred to the wind turbine rotor is reduced by $C_p$. The extracted mechanical power from the turbine is given by:

$$P_m = \frac{1}{2}\rho\pi r^2 V_w^3 C_p \tag{5}$$

$$\lambda = \frac{\omega_m r}{V_w} \tag{6}$$

The wind turbine mechanical torque can be expressed as:

$$T_m = \frac{P_m}{\omega_m} = \frac{\rho\pi r^2 V_w^3 C_p}{2\omega_m} \tag{7}$$

### 2.3 Electrical modelling

The electrical modelling used in this work is that of a DFIG. A model of the electrical machine which is adequate for designing the control system must preferably incorporate all the important dynamic effects occurring during steady state and transient operations [18,19]. The following equations describe the circuit representing a standalone DFIG application. In electrical modeling, direct–quadrature–zero (*dq*0) transformation is a mathematical transformation that rotates the reference frame of three-phase systems in an effort to simplify the analysis of three-phase circuits. Using Park's transformation (from *abc* frame to *dq* reference frame) [20], the machine equations describing the dynamics are

Voltage equations:

$$v_{ds} = -R_s i_{ds} - \omega_s\lambda_{qs} + \frac{d\lambda_{ds}}{dt} \tag{8}$$

$$v_{qs} = -R_s i_{qs} + \omega_s\lambda_{ds} + \frac{d\lambda_{qs}}{dt} \tag{9}$$

$$v_{dr} = -R_r i_{dr} - s\omega_s\lambda_{qr} + \frac{d\lambda_{dr}}{dt} \tag{10}$$

$$v_{qr} = -R_r i_{qr} + s\omega_s\lambda_{dr} + \frac{d\lambda_{qr}}{dt} \tag{11}$$

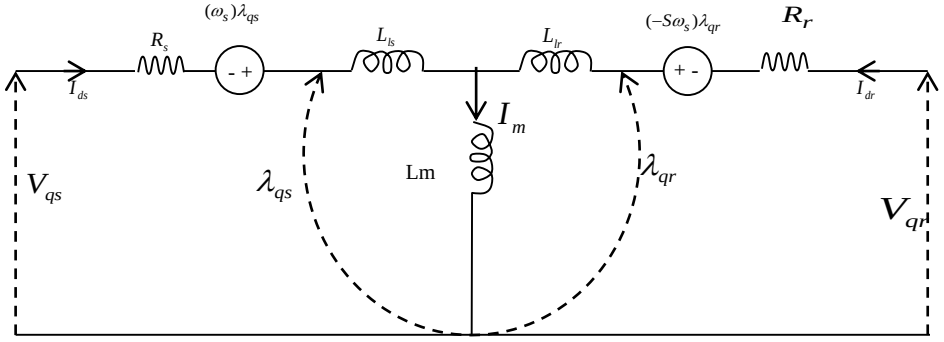


Figure 2. Equivalent circuit diagram of the electrical representation of the DFIG

Flux linkages equations:

$$\lambda_{ds} = -(L_s + L_m)i_{ds} - L_m i_{dr} \tag{12}$$

$$\lambda_{qs} = -(L_s + L_m)i_{qs} - L_m i_{qr} \tag{13}$$

$$\lambda_{dr} = -(L_r + L_m)i_{dr} - L_m i_{ds} \tag{14}$$

$$\lambda_{qr} = -(L_r + L_m)i_{qr} - L_m i_{qs} \tag{15}$$

Rotor slip:

$$s = \frac{\omega_s - \omega_r}{\omega_s} \tag{16}$$

$$\omega_s = \frac{2\pi}{60} N_s \tag{17}$$

$$N_s = \frac{120fs}{P} \tag{18}$$

Neglecting the stator resistance and assuming that the *d*-axis coincides with the maximum of the stator flux results in the electrical torque equation as

$$T = \frac{3}{2}\left(\frac{P}{2}\right)\left(\lambda_{dr} i_{qr} - \lambda_{qr} i_{dr}\right) = \frac{3}{2}\left(\frac{P}{2}\right) L_m\left(i_{qs} i_{dr} - i_{ds} i_{qr}\right) \tag{19}$$

Active power injected into the grid is expressed as

$$P = v_{ds} i_{ds} + v_{qs} i_{qs} + \left(v_{dr} i_{dr} + v_{qr} i_{qr}\right)\eta_{conv} \tag{20}$$

The vector control of the DFIG is achieved using basic Park's and Clark's transformations, from *abc*-D/Q-*d/q*, to alpha-beta. However, in the grid connected three-phase inverter, *dq* transformation in synchronous reference frame is used to simplify the control algorithm. As the input signals are transformed to dq frame, these signals are transformed to DC quantities. Due to this, signals are easily regulated to their reference values by using PI controller. Generally, in this control *d*-component is responsible to control active power and *q*-component is used for reactive power control.

The dq transformation at the synchronous reference frame allows time-varying sinusoidal signals to be transformed into stationary signals which simplify the control of three-phase inverters. For three-phase inverters, usually the *d*-axis is in line with the terminal voltage, and the phase locked loop (PLL) regulates *Vq* to zero. Hence all the voltage appears on the *d*-axis: Vd ~ 1 p.u., the *d*-axis current corresponds to active power and the *q*-axis to reactive power. Another convention involves places the *q*-axis in line with the terminal voltage of the three-phase inverter which means that the situation is reversed: *d*-axis current is reactive and *q*-axis current corresponds to active power. In summary, depending on the transformation matrix used for controlling the system, function of *d* and *q* components can be interchanged. The parameters of the machine and other component values used for simulation are presented in Table 1.

Table 1. Machine parameters and component dimension

| **Machine elements** | **Values** | **Grid side converter** | **Values** |
|---|---|---|---|
| Number of poles | 4 | DC bus capacitance | $800 \times 10^{-3}$ |
| Rotor resistance | $2.9 \times 10^{-3}$ Ω | Filter resistance | $20 \times 10^{-6}$ H |
| Stator resistance | $2.6 \times 10^{-3}$ Ω | Filter inductance | $400 \times 10^{6}$ H |
| Leakage inductance of stator | $0.087 \times 10^{-3}$ H | Radius of blade | 42 m |
| Magnetizing inductance | $2.5 \times 10^{-3}$ H | Gear ratio | 100 |
| Rated Voltage | 2070 V | Pitch angle | 0 |
| Rated frequency | 50 Hz | Air density | 1.225 kg/m$^3$ |
| Stator power | $2 \times 10^{6}$ W | Wind velocity | 8.5 m/s |
| Rated speed | 1500 rpm | Crow bar resistance | 0.2 Ω |
| Rated stator voltage | 690 V | | |
| Rated stator current | 1760 A | | |
| Rated torque | 12732 Nm | | |

## 3. SIMULATION RESULTS AND DISCUSSION

A MATLAB/Simulink software is used to implement the simulation study. Figure 3 shows the simulation diagram, while Figures 4 and 5 show the Simulink models of the rotor side and grid side, converters control respectively.

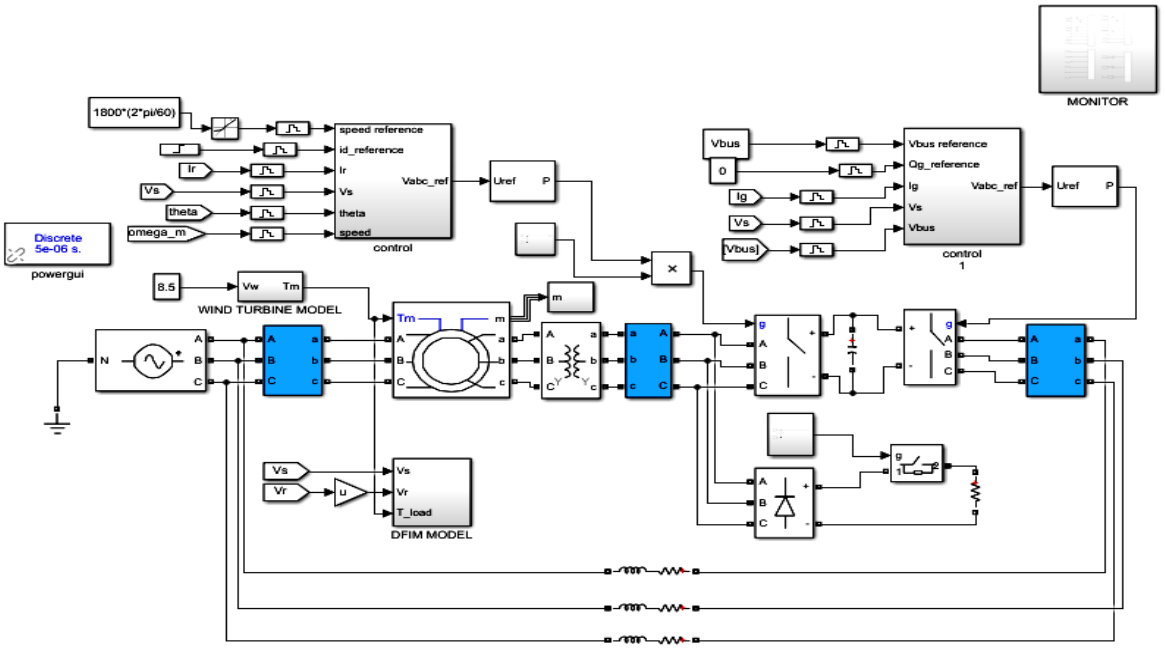


Figure 3. Simulation diagram of a DFIG

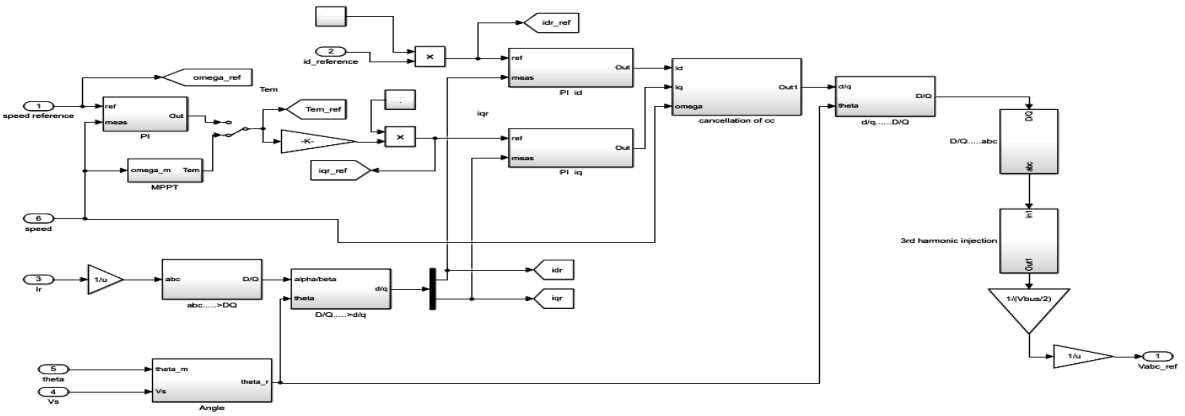


Figure 4. Simulink model of rotor side converter control

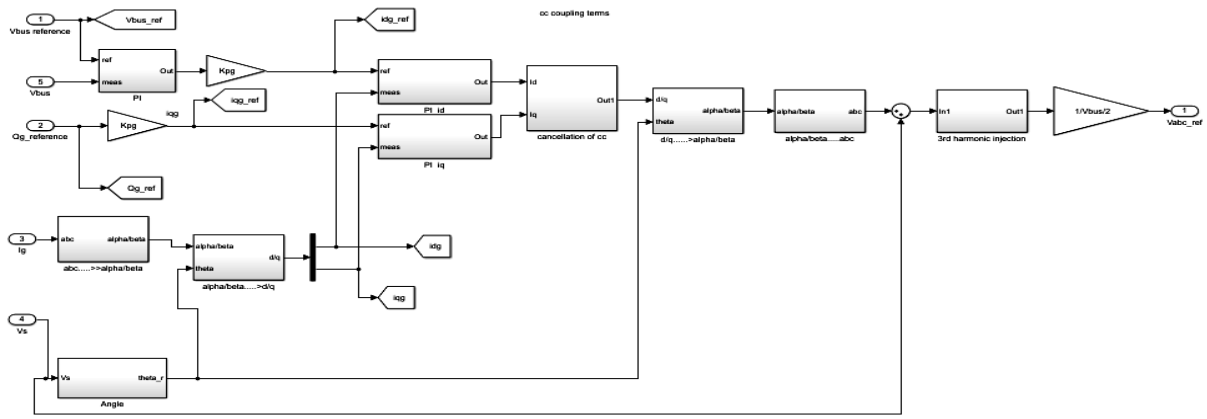


Figure 5. Simulink model of grid side converter control

After performing the simulations, several responses were obtained. Figure 6 presents the relationships between the $\lambda$ and *Ct* and also the power and the wind speed. The maximum may be in the neighborhood of 0.57. Also at the speed of 10 m/s is almost associated with about 1.5 MW. From Figure 7, and at the rotor side, it is observed that about half the rated speed, there was a drift in the torque, a consequent of the current, the stator phase voltages are 120° apart. Figure 8 shows that the voltage output was steady with its magnitude above 100 V. At about 1.7 s when the current *Ig* is vanishing corresponds to the time that the quadrature voltages and current are stabilizing. From Figure 9, the fault values were reduced, but however increased as it approaches the fourth second. In Figure 10, the associated ripples of the DFIG output are attendant manifestations of the effect of unsteady energy flow via the DC link capacitors. At wind speed of 2 m/s, an analytical model of the DFIG gave the responses from the rotor side and grid side controls as well as responses from the fault analysis and DFIG model. Due to transformation, each stated characteristics was plotted against the per unit time.

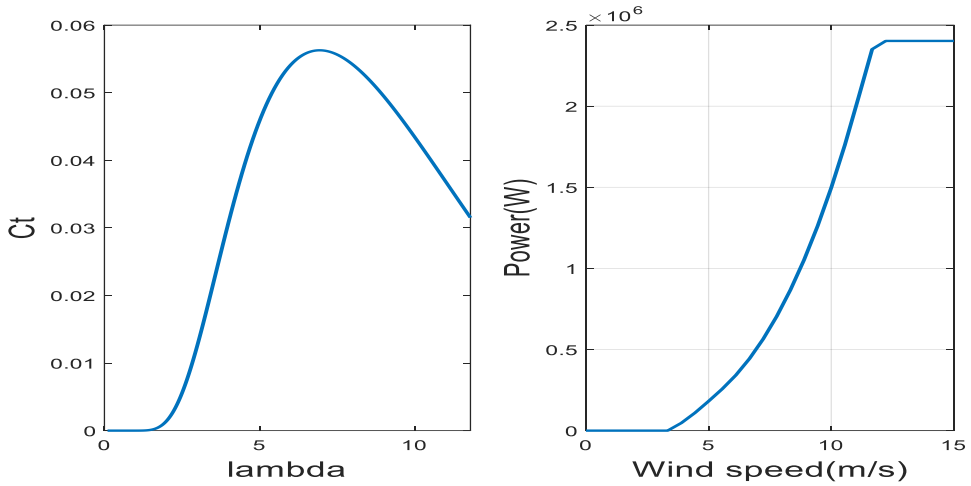


Figure 6. Curve of power against wind speed

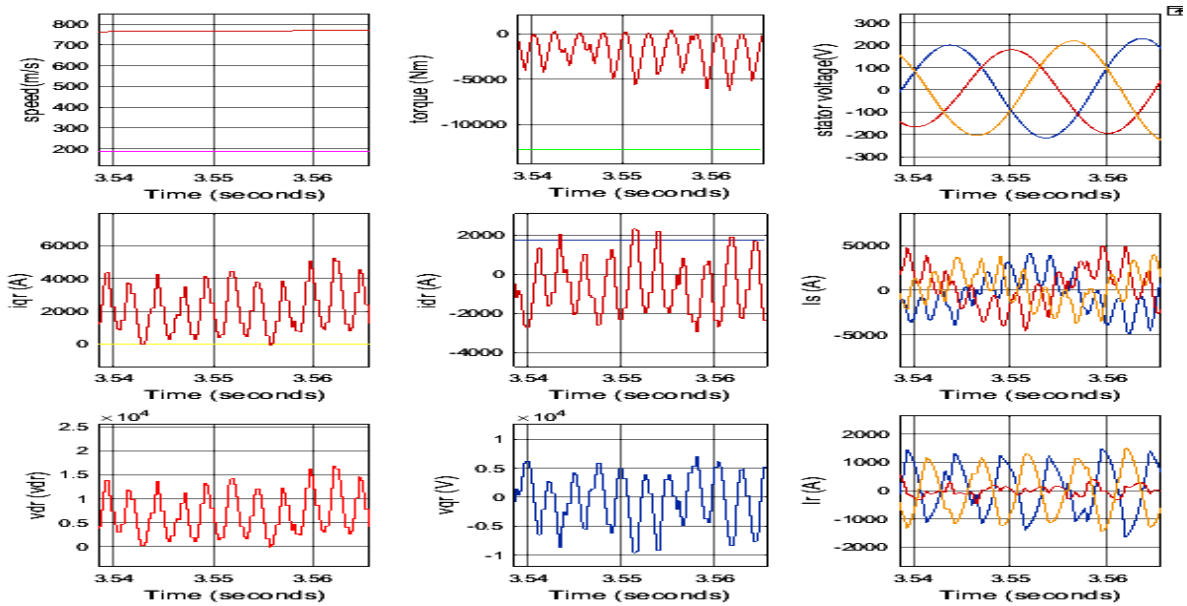


Figure 7. Output from the rotor side control

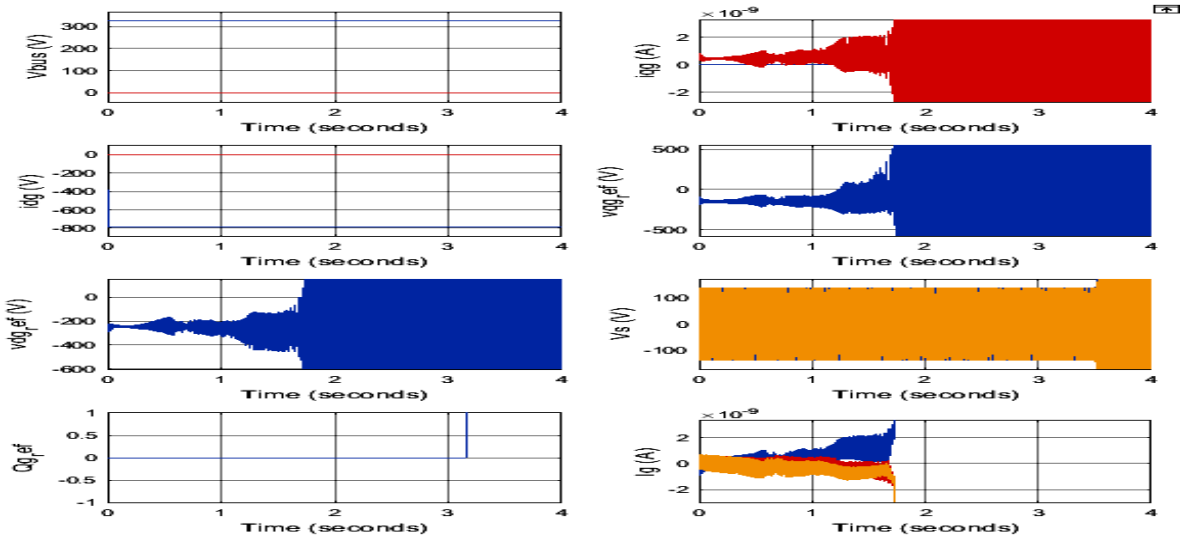


Figure 8. Output from the grid side control

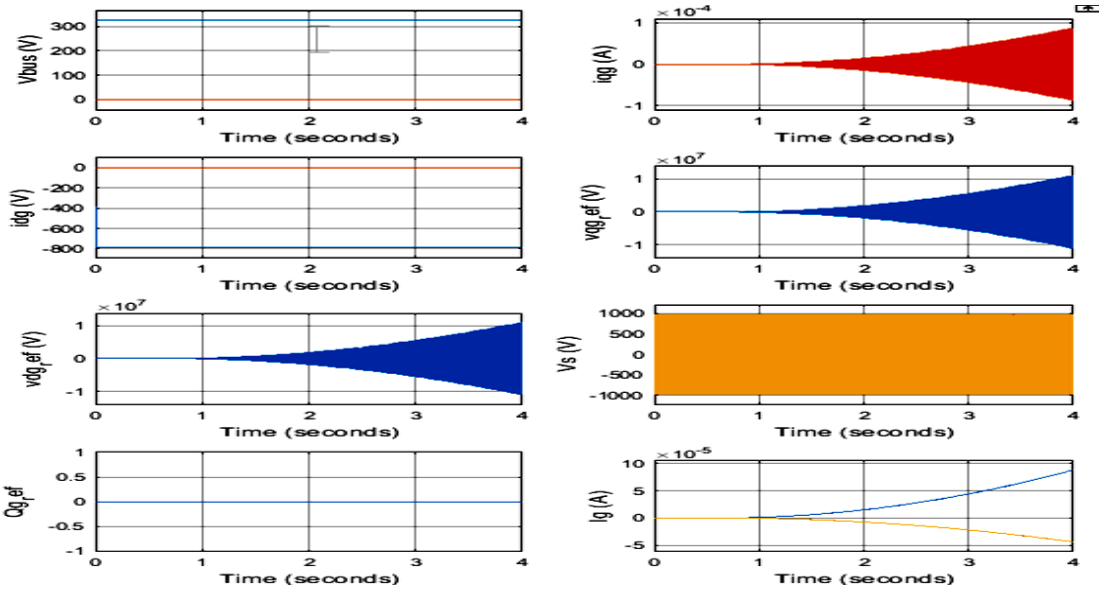


Figure 9. Output from the fault analysis

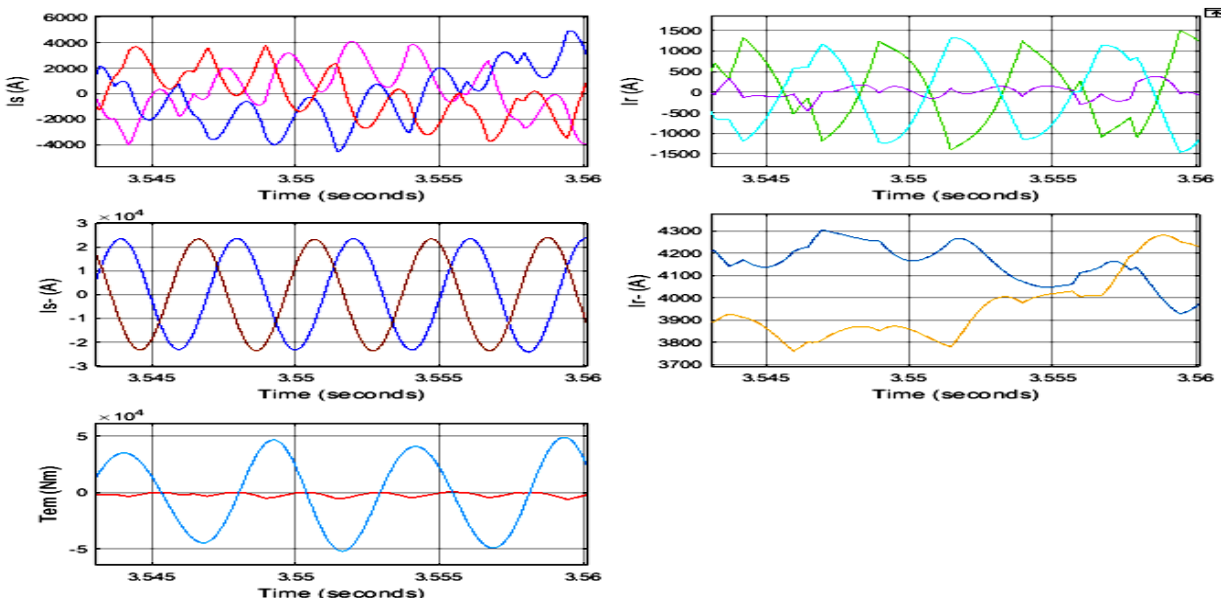


Figure 10. Output of the DFIG model

From Figure 7, and at the rotor side, it is observed that about halve the rated speed, there was a drift in the torque, a consequent of the current, the stator phase voltages are 120 degrees apart. From Figure 8, the voltage output is observed to be steady with its magnitude above 100V. At about 1.7s when the current Ig is vanishing corresponds to the time that the quadrature voltages and current are stabilizing. From Figure 9, the fault values were reduced but however increased as it approaches the fourth second. In Figure 10, the associated ripples of the DFIG output are attendant manifestations of the effect of unsteady energy flow via the DC link capacitors. At wind speed of 2 m/s, an analytical model of the DFIG gave the following responses from the rotor side and grid side controls as well as responses from the fault analysis and DFIG model. Due to transformation each stated characteristics is plotted against the per unit time.

To establish case for comparison, at wind speed of 8.5 m/s, an analytical model of the DFIG gave the responses from the rotor side and grid side controls as well as responses from the fault analysis and DFIG model as shown in Figures 11-14. From Figure 11, and at the rotor side, it is observed at the constant speed of 1500rad/seconds there was an attendant decrease in the torque as can be seen from the graph, also a consequent of the current. The stator voltage phase components maintained the 120° as expected. From Figure 12, the bus or source voltage output is observed to be steady while the quadrature components of the current and voltage started increasing appreciably from about 1.5 s. From Figure 13, the fault values were further reduced but not as much as it approached the fourth second. In Figure 14, the output of the DFIG is far better than what was earlier got from Figure 10. In view of the assertions, it is due to note that, the parameters of the system changes with change in wind speed which indicated that there will be no power generated at very low or zero wind speed. An average wind speed of about 8.5 m/s is seen to generate a considerable voltage and current. Due to the control of the rotor side, the doubly fed induction machine is properly controlled to desirable quality. At wind speed of about 2 m/s, the amount of voltage generated is seen not to compare favourably to the voltage generated at 8.5 m/s.

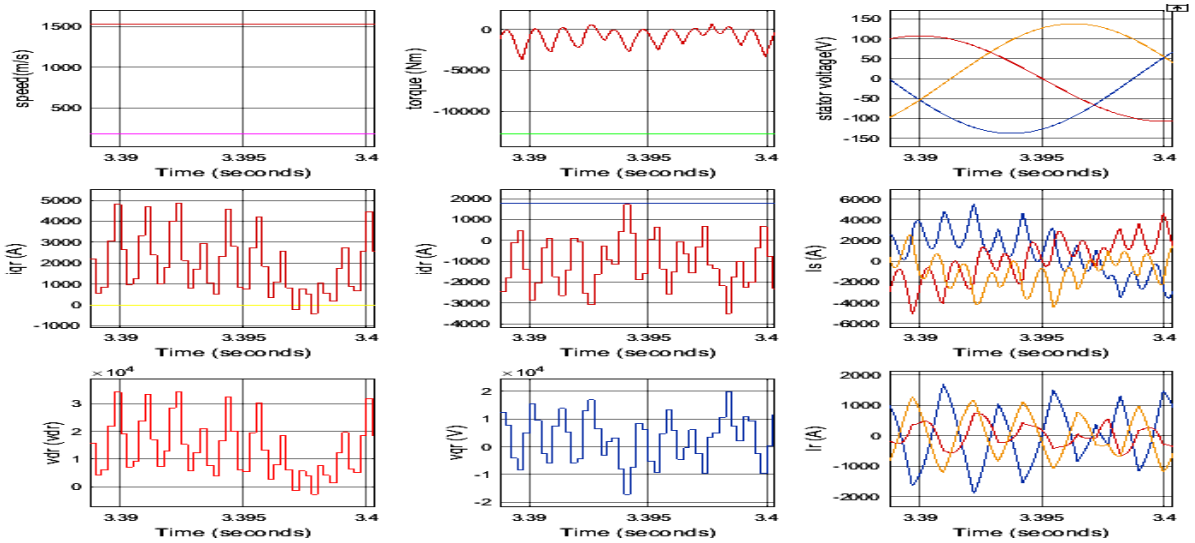


Figure 11. Output from the rotor side control

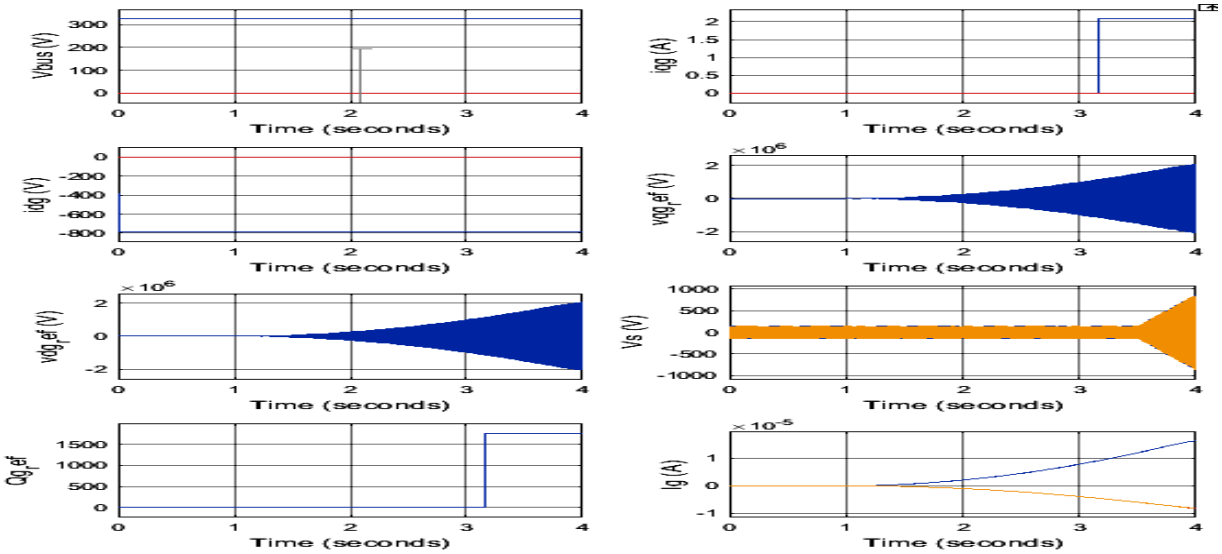


Figure 12. Output from the grid side control

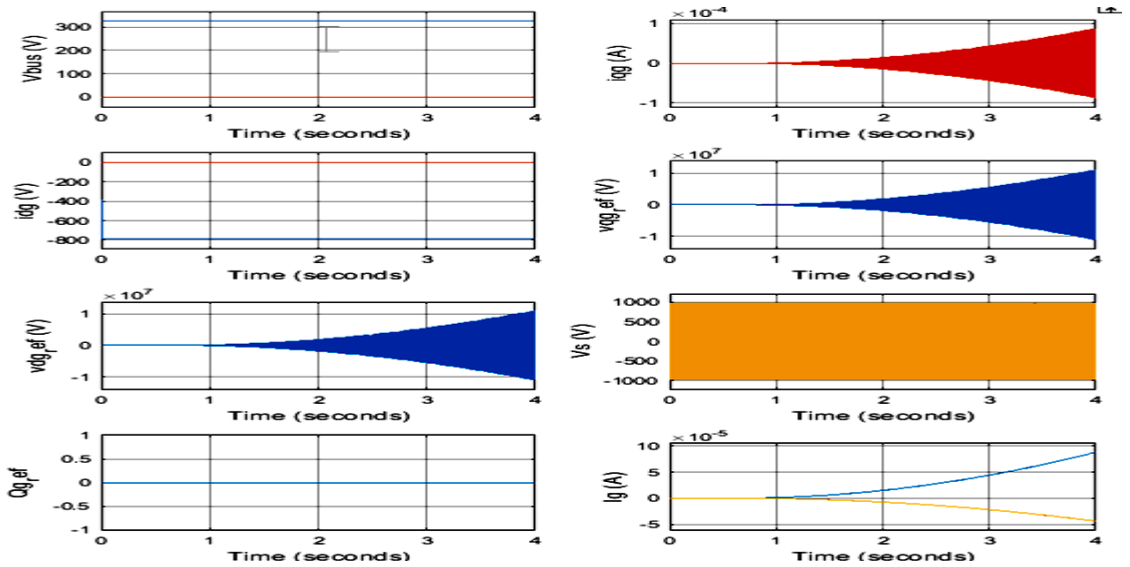


Figure 13. Output from the fault analysis

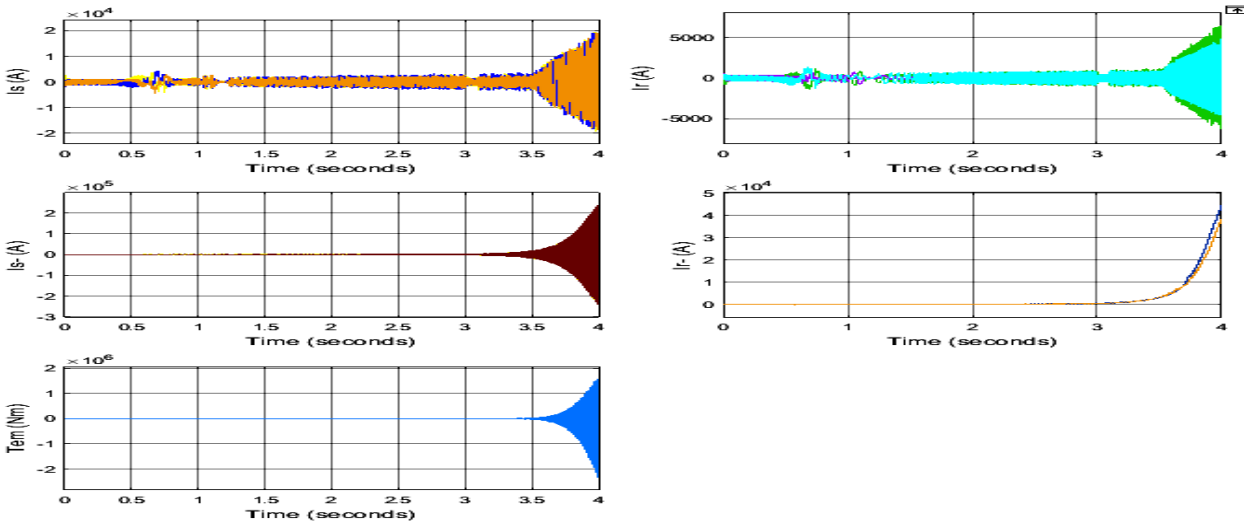


Figure 14. Output of the DFIG model

## 4. CONCLUSION

Wind energy system can be incorporated into electric grid for maximum and reliable power supply. It is a reliable source of energy, also environmental friendly, notwithstanding the seasonal and other dynamics associated with this source of power, such as change in wind speed, cost of installation, etc. The doubly-fed induction machine is a wound-rotor doubly-fed electric machine and has several advantages over a conventional induction machine in wind power applications. First, as the rotor circuit is controlled by a power electronics converter, the induction generator is able to both import and export reactive power. This has important consequences for power system stability and allows the machine to support the grid during severe voltage disturbances (low-voltage ride-through; LVRT). Second, the control of the rotor voltages and currents enables the induction machine to remain synchronized with the grid while the wind turbine speed varies. A variable speed wind turbine utilizes the available wind resource more efficiently than a fixed speed wind turbine, especially during light wind conditions. Third, the cost of the converter has according to [16] been known to be low when compared with other variable speed solutions because only a fraction of the mechanical power, typically 25–30%, is fed to the grid through the converter, the rest being fed to grid directly from the stator. In summary, the following are the benefit; constant frequency output signal to the grid irrespective of the variable rotor speed, low power rating required for the power electronic devices and hence low cost of control system, power factor is controlled, i.e. maintained at unity, electric power generation at low wind speed, power electronic converter has to handle the fraction of the total load i.e., 20-30% and also cost of this converter is low than in case of the other types of generators.

**REFERENCES**


[1] S. Nagashima, Y. Uchiyama and K. Okajima, Environment, energy and economic analysis of wind power generation system installation with input-output table, *Energy Procedia*, 75, 683-690, 2015.

[2] A. K. Azad, M. G. Rasul, R. Islam and I. R. Shishir, Analysis of wind energy prospect for power generation by three Weibull distribution methods, *Energy Procedia*, 75, 722-727, 2015.

[3] B. O. Bilal, M. Ndongo, C. M. Kebe, V. Sambou and P. A. Ndiaye, Feasibility study of wind energy potential for electricity generation in the northwestern coast of Senegal, *Energy Procedia*, 36, 1119-1129, 2013.

[4] D. K. Kidmo, K. Deli, D. Raidandi and S. D. Yamigno, Wind energy for electricity generation in the far north region of Cameroon, *Energy Procedia*, 93, 66-73, 2016.

[5] D. J. Allen, A. S. Tomlin, C. S. E. Bale, A. Skea, S. Vosper and M. L. Gallani, A boundary layer scaling technique for estimating near-surface wind energy using numerical weather prediction and wind map data, *Applied Energy*, 208, 1246-1257, 2017.

[6] A. Akintayo and W. Zhou, A preliminary analysis of wind turbine energy yield, *Energy Procedia*, 138, 423-428, 2017.

[7] C. Sranpat, S. Unsakul, P. Choljararux and T. Leephakpreeda, CFD-based performance analysis on design factors of vertical axis turbines at low wind speeds, *Energy Procedia*, 138, 500-505, 2017.

[8] A. Zanon, M. De Gennaro and H. Kuhnelt, Wind energy harnessing of the NREL 5 MW reference wind turbine in icing conditions under different operational strategies, *Renewable Energy*, 115, 760-772, 2018.

[9] J. B. Gupta, *A Course in Power System*, S. K. Kataria and Sons, 2013.

[10] P. Jain, *Wind Energy Engineering*. The McGraw-Hill Companies, 2011.

[11] T. Burton, D. Sharpe, N. Jenkins and E. Bossanyi, *Wind Energy Handbook*. John Wiley and Sons Ltd, 2001.

[12] J. F. Manwell, J. G. McGowan and A. L. Rogers, *Wind Energy Explained Theory, Design and Application*. John Wiley and Sons Ltd, 2009.

[13] M. A. Abomahdi and A. K. Bharadwaj, Modeling and simulation of DFIG to grid connected wind power generation using matlab. https://www.researchgate.net/publication/298845736 (accessed 10.9.2019).

[14] C. Hamon, K. Elkington and M. Ghandhari, Doubly-fed Induction Generator Modeling and Control, *2010 International Conference on Power System Technology*, Hangzhou, 2010, pp. 1-7.

[15] N. Kumari, A. N. Jha and N. Malik, Development of wind power generation model with DFIG for varying wind speed and frequency control for wind diesel power plant, *International Journal of Engineering and Technology*, 8(2), 596-603, 2016.

[16] Doubly-Fed Electric Machine. https://en.wikipedia.org/wiki/Doubly-fed_electric_machine (accessed 10.10.2019).

[17] J. Fletcher and J. Yang, Introduction to the doubly-fed induction generator for wind power applications, *Paths to Sustainable Energy*, 259-278, 2010.

[18] P. Vas, *Vector Control of AC Machines*. Oxford University Press, 1990.

[19] X. Jing, *Modeling and control of a doubly-fed induction generator for wind turbine-generator systems*, Master Thesis, Marquette University, 2009.

[20] P. Krause, O. Wasynczuk and S. Sudhoff, *Analysis of Electric Machinery and Drive Systems*. NJ: IEEE Press, 2002.